PIRE-GEMADARC Internal Notes – Germanium Internal Amplification (GeIA):
*

Chih-Hsiang Yeh
Institute of Physics, Academic Sinica, Nangang, Taipei, Taiwan and
Department of Physics, National Central University, Chungli, Taoyuan, Taiwan†
(PIRE-GEMADARC Collaboration)
(Dated: April 6, 2021)

To understand the solid-state physics emerging in the crystal for the germanium internal amplification at two conventional temperatures, which are liquid nitrogen temperature(77K) and liquid helium temperature(4K), some of the literature studies are completed with the content summarized in this note.

CONTENTS

I. INTRODUCTION

Since some of the experiments, such as the low-mass WIMP search with χN scattering, require the low-threshold detector for detecting the small amount of energy, the fundamental laws of internal amplification, which can be utilized for enlarging the signal directly, should be revealed for getting it to be manageable.

In 2000, two experts from Russian, who are the pioneers of our research, came up with the conceptual design about applying the high voltage on the Ge detector, along with the electron-hole pairs that can be enhanced within the avalanche region showing up in the crystal. Thereby, there are a bunch of experiments having an attempt to extend the idea and to see whether it can be worked out with the state-of-the-art technology in reality.

In our collaborations, two teams are realizing the notion under two conventional temperatures, which are 4K(USD) and 77K(THU). Under these two different temperatures, the phenomenon happening to the signal and noise in the crystal would be disparate. The studies are expected to carry out the difference between these two setups, and the advantage versus disadvantage in a variety of facets to them.

In the following sections, first, some of the basic knowledge related to the p-n junction would be conducted as the foundation of this research. Then, under these two temperatures mentioned previously, the internal amplification on the signal will be elaborated on. In parallel, as the signal is strengthened, the noise of the crystal could be unexpectedly magnified consequently. Dealing with the adversity of the high noise originating from three species of leakage currents in the crystal is the very next topic that should be addressed. After all, the signal-to-noise ratio is the ultimate criteria to compare between different setups.

At the end of the notes, first the calculation of the gain factor, which is based on the authentic electric field distribution in the P-type point contact(PPC) detector, would be regarded. Hereafter, in practical, because of the thorny problem on the dielectric breakdown, which is due to the tremendously high electric field and can sabotage the crystal intrinsically for both temperatures, the mechanism of that would be delivered to assess the crucial voltage on protecting the crystal from being destroyed.

*
† a9510130375@gmail.com

II. BASIC P-N JUNCTION

Given the semiconductor containing the different types of impurity, two groups, including the n(electron-dominant) and p(hole-dominant) types, can be characterized. For any crystal containing both types of semiconductors, the properties of the p-n junction will occur. The phenomenon for it would be discussed as follows.

In Fig.1, the typical p-n junction is illustrated. On the p-n junction, the electron-hole diffusion, as well as the attraction, will start emerging in the crystal. After the "dynamic" get balance, the neutral region called "the depletion region", which the stable electric field flows in, will show up. In the reverse-bias case, the higher the voltage, the larger the region it will be. In the end, the voltage should be enhanced to the one which can deplete the whole crystal, implying all electrons and holes in the crystal get equilibrium. Afterward, the application of this "neutral" crystal can start off.

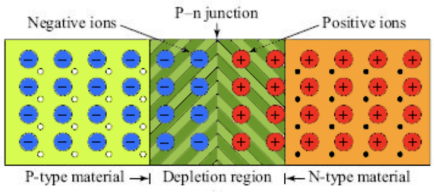

The PN junction is the region between the p and n-type material

FIG. 1. The basic P-N Junction.

Then, the voltage, which is applied to fully deplete the crystal, can be derived from the formula as follows:

$$x_d = \sqrt{\frac{2\epsilon V_d}{qN_a}} \tag{1}$$

x_d is the depletion length as obtained from the crystal, N_a is the impurity concentration, V_d is the voltage solicited to do the task of the depletion. After moving some of the parameters from right to left, then the depletion voltage can be demonstrated clearly:

$$V_d = \frac{x_d^2 q N_a}{2\epsilon} \tag{2}$$

In FIG.2, the depletion voltage under the various temperatures for a detector with a length of 2.37cm is displayed. When the temperature becomes lower, the depletion voltage will be decreased.

If the details of it about the fundamental physics in semiconductor is desired, chapter7 and chapter8 of the book[1] are recommended.

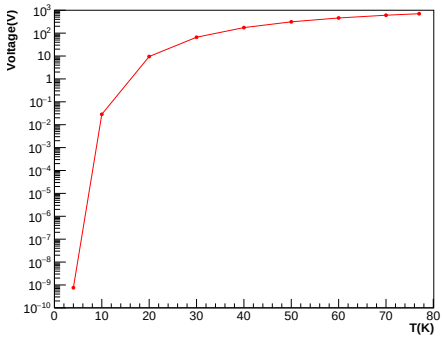

FIG. 2. The depletion voltage as a function of the temperature for the detector with the length equal to 2.37cm.

III. SIGNAL AMPLIFICATION

A. Necessary Parameters from "an electron":

At the start, let us visualize "an electron", which is ionized by a WIMP, flowing in the crystal. Many necessary parameters must be acquired in advance from this electron to unfold our studies. All of them will be depicted in the following subsections.

1. *Electrical Mobility(μ)*

From the definition of electrical mobility, which is as follows:

$$\mu = \frac{V_d(1 + \frac{E}{E_{sat}})}{E} \tag{3}$$

V_d is the velocity of the electron, and E is the electric field applied to the crystal.

The mobility is estimated by the formula above. Specially, since in our experiment, the ultra-high electric field is applied, the saturation phenomenon, referring to the situation that the velocity would be a constant when the electric field is beyond the critical one, can be obtained. In Fig.3[2], when the electric field is upon 10^4V/cm, which is also the critical electric field in calculating the ionization rate described in the latter section, the velocity of the electron is a constant for both temperatures.

2. *Effective mass(m*)*

Under the different temperatures, the effective conductivity masses are various. In Fig.4[3], the hole has the higher effective mass when the temperature is low. BTW, since there is no such study for Ge, Si study is taken as an instance to picture the tendency of the effective masses for the electron and the hole. In our studies, the effective mass for the electron is simply set at m =

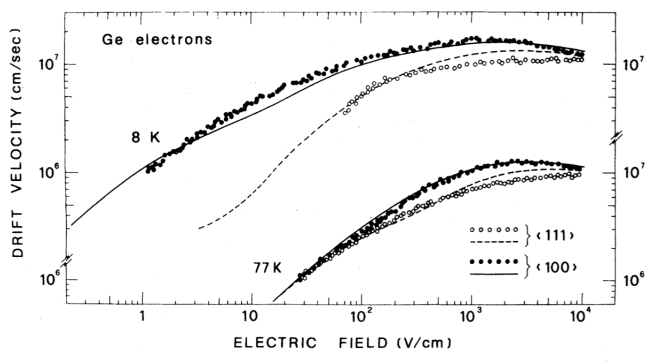

FIG. 3. The drift velocity as a function of electric field is shown for the different temperatures.

0.12m0 and for the hole, the effective mass is simply set at m=0.21m0.

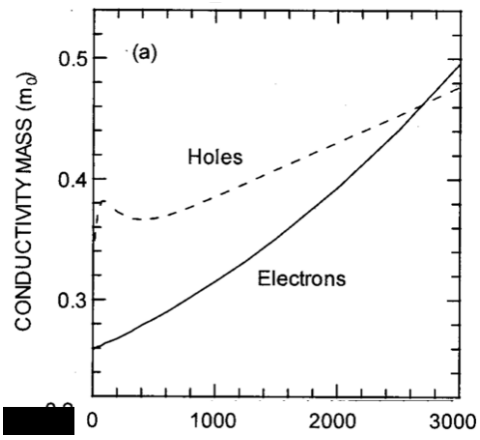

FIG. 4. The relation between the effective mass(m_0) and the temperature(T) is demonstrated for both electron/hole in Si.

3. *Relaxation Time(τ)*

The period of time that the electron can survive without bumping into another atom:

$$\tau = \frac{\mu \times m*}{e} \tag{4}$$

e is the coulomb constant, μ is the mobility of the electron, and m* is the effective mass.

After acquainting the relaxation time, the next thing that should be figured out is the mean free path(L), which means how far the electron can go along without ramming with another atom in the crystal. The formula is as follows:

$$L = \tau \times V_d \tag{5}$$

V_d means the velocity of the electron, and τ is the relaxation time.

After all of the parameters are well-recognized in this section, those would be made use of in the next section for developing the theory of amplifying the signal.

B. Real beef: Ionization rate

The ionization rate is defined as the following description: How many electrons/holes can be ionized within 1cm?

After depleting the crystal, next the relation between the ionization rate and the E(V/cm) can be brought to light. Based on the formulae (6),(7) and (8) from paper[4], the ionization rate can be decided by exploiting the mean free path(L), electric field(E(x)) and ionization energy(U) of the material,

$$\alpha_s = \frac{a_s}{z} exp(-\frac{b_s}{E(x)}) \tag{6}$$

$$z(x) = 1 + \frac{b_n}{E(x)} exp(-\frac{b_n}{E(x)}) + \frac{b_p}{E(x)} exp(-\frac{b_p}{E(x)}) \tag{7}$$

$$a_s = \frac{1}{L_s}, b_s = \frac{U_s}{qL_s}, s = (p,n)type \tag{8}$$

α_s means the Ionization rate, E(x) is the electric field distributing in the crystal, L_s is the mean free path[5], and U_s means the Ionization energy, which is set to be 3eV as measured in this paper[6].

The FIG.5 can be framed by employing the formulae introduced above. From this scheme, there are three important pieces of information that can be concluded:

1. Critical E=10^4 V/cm
2. The significant difference between e/h cases is the effective mass under such high electric field at the same T.
3. Hole can give us more signal under 4K.

C. Pioneer: Russian investigation[2000]

In light of the paper[7], the conceptual design on the coaxial detector HPGe, which is displayed in FIG.6, is provided. In order to estimate the gain factor, which is a

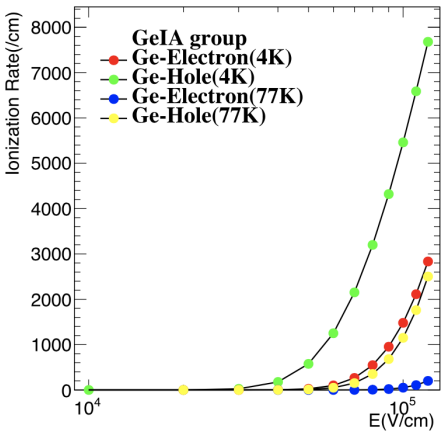

FIG. 5. The ionization rates for both electron and hole under both 4K and 77K.

criteria for the performance of the detector as described in the end of this note, the electric field distributing in the detector should be recognized beforehand. The distributions in the strip detector can be illustrated with the impurity concentration as the following formula:

$$E(r) = \frac{Ne}{2\epsilon} r - \frac{V + \frac{Ne}{4\epsilon}(R_2^2 - R_1^2)}{r \ln(\frac{R_2}{R_1})} \tag{9}$$

where N is the impurity concentration, e is the electron charge, ϵ is the dielectric constant of the germanium, R_2 and R_1 are the radii of the cathode and the anode, and V is the applied voltage.

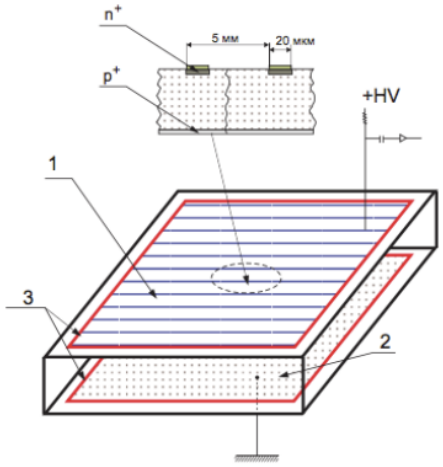

FIG. 6. Germanium detector with an internal amplification (schematic view): (1) anode strips, (2) cathode, and (3) guard electrodes. The scheme of n+ and p+ layers is shown in the upper part of the figure.

According to FIG.5, when the electric field is higher than 10^4(V/cm), the electron will be increased as the function of the electric field. As a result of that, after the electric fields with the different impurity concentrations are demonstrated in FIG.7[7], which is based on the calculation by the formula(9), two regions can be separated with this critical electric field.

1. Avalanche region: When the electric field is above 10^4(V/cm), the avalanche effect will emerge, subsequently, the signal will be amplified.

2. Reach-through region: If the electric field is below the critical one, then the electron/hole will just go through normally without any effect.

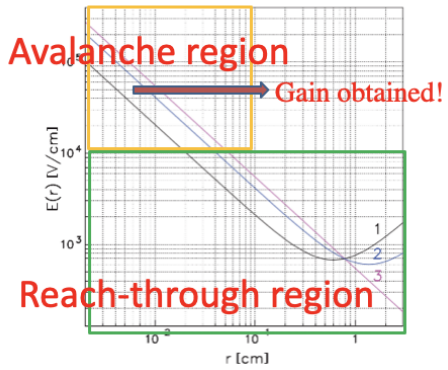

FIG. 7. The electric field as a function of the distance from the strip in FIG.6 with the different impurities. The numbers above the lines mean the different impurities: (1)$10^{10} cm^{-3}$, (2)$4 \times 10^9 cm^{-3}$ and (3) 0 cm^{-3}

These studies give out a clue that the detector can be devised to yield the amplification for the signal with the electric field above a certain level.

IV. NOISE IN THE CRYSTAL

Unfortunately, the noise in the crystal is inevitable. The genres of the noise in the crystal should be characterized as the criteria of the limitation of measuring the lowest mass for dark matter theoretically. There are three sorts of noise in the crystal, encompassing the bulk leakage current, the contact leakage current, and the surface leakage current. In the following paragraph, all of them are described individually.

A. Bulk leakage current

Due to the thermal fluctuation, the electrons from the bulk(purity, such as Ge) material will be ionized possibly. Fortunately, the level of this noise can be ignored below

77K. The associated information is well-written in the formula(13)[8]:

$$I = Ae^{\frac{-E_{\text{Ge Band}}}{2k_BT}} * q * \frac{1}{t} \tag{10}$$

A is the intrinsic concentration, $E_{\text{Ge Band}}$ is the band gap of Ge, q is the coulomb constant, T is the temperature(K), and t is the period of the time the electron/hole would come to the detector.

B. Contact leakage current

Because of

1. Barrier between the semi-metal connection
2. Thermal fluctuation

There is a possibility that the electron in the conductive band could leap into the metal, leading to the dark current which is unwanted.

In Fig.8[9], which is the measurement from USD, gives out the thread about the scale of the contact leakage current at 100K is around $5 \times 10^{-10} A/cm^2$. Compared with our result, the Fig.9[10], which is demonstrated by other group with the a-Ge detector, also has the similar results at 100K. Upon the usage of FIG.9, the contact leakage current under 77K, which is around $5 \times 10^{-16} A/cm^2$. can be extrapolated.

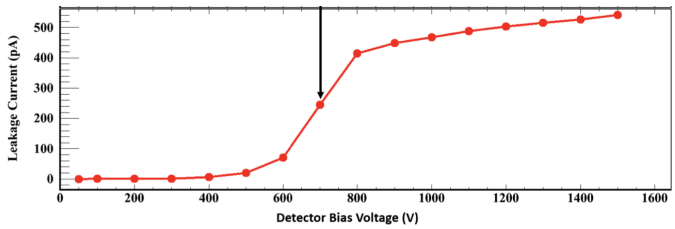

FIG. 8. The determination of full depletion voltage for detector USD-L01 using I-V measurements at 100 K.

The fundamental physics is "Schottky effect", which is a kind of the thermal emission. The simplified formula can be expressed with the "Richardson's law" as follows:

$$I \propto T^2 e^{\frac{W}{k_BT}} \tag{11}$$

$E_{\text{Ge Band}}$ is the band gap of Ge, q is the coulomb constant, T is the temperature(K), W is the work function of the material, and A is the measured constant.

The detail of this mechanism is compiled in the book[11]. Basically, it is a Metal-Semiconductor junction problem, which is a very big topic authentically and the chapter 10, 11 of book[11](Strongly recommended!) and chapter 6 and 7 of book[12] are recommended to acquire more detail on the related topic.

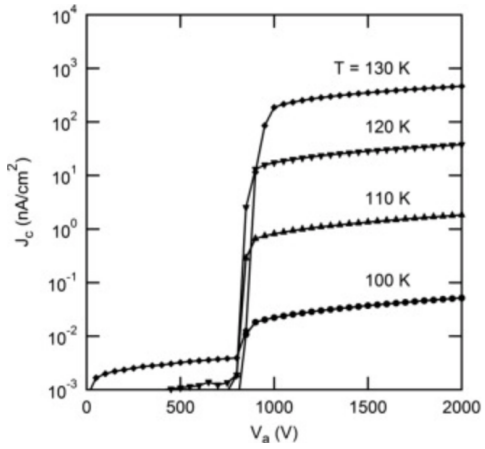

FIG. 9. Measured center contact leakage current density plotted as a function of bias voltage at various temperatures for an a-Ge/HPGe/a-Ge detector

C. Surface leakage current

It depends on the quality of the crystal. By and large, lowering the temperature can help get rid of the noise.

There are two papers depicting the measurement of the surface leakage current for Ge. Please look at Fig.10[13], which shows the surface leakage current from InAs Avalanche Photodiodes. Although this is not for Ge, it gives us a hint on the scale of the semiconductors. The points(■) can be expanded in the figure to predict the surface leakage current under more lower temperatures. The extremely low surface leakage current can be inferred in this paradigm under the low temperature.

Currently, the new results of a-Ge for the surface leakage current from USD are published. Amazingly, In FIG.11[14], the leakage current is projected down to the temperature at 4K, and the considerably low leakage current is illustrated at the very low temperature, leading to the feasibility of detecting the low-mass dark matter.

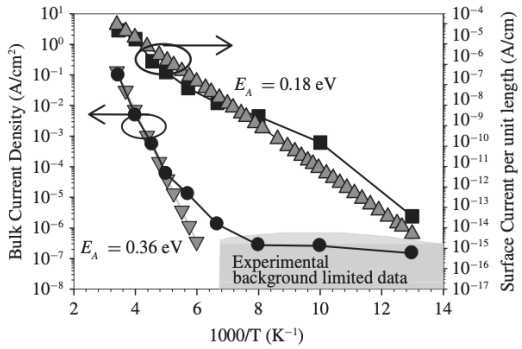

FIG. 10. The surface leakage current, which is remarked by (■), is measured with the InAs Avalanche Photodiodes.

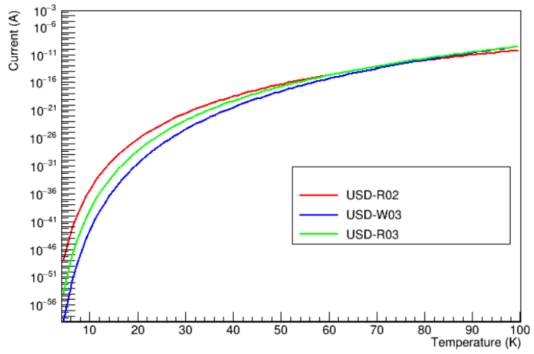

FIG. 11. Projected variation of the surface leakage current with temperature for a PPC detector using the parameters obtained for the a-Ge used in detectors USD-R03, USD-R02 and USD-WO3. .

D. Summary for three currents

In FIG.12, the chart for summarizing these three currents under the saturation circumstance are displayed. Overall, the surface leakage current is the severe conundrum for any temperature. At 77K, the contact leakage current is competitive with the surface leakage current, as their numbers are very close to each other. At 4K, surprisingly, the surface leakage current surpasses all others overwhelmingly.

V. PERFORMANCE FOR THE DETECTOR

In this section, the performance of the detector is expected to be projected under both temperatures with the information at hand.

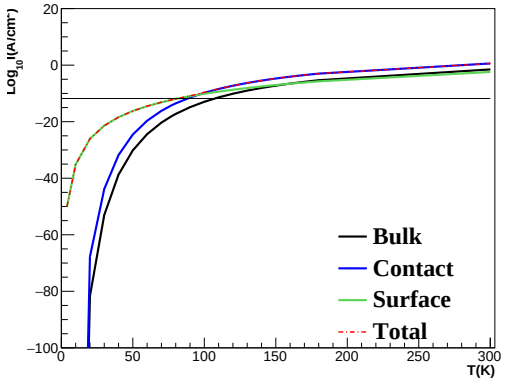

FIG. 12. The leakage current as a function of the temperature for three types of leakage currents.

A. Gain

The gain factor can be estimated with two parameters, including the electric field and the ionization rate. Given the geometry of the detector, the gain factor can be obtained:

$$G = \int \alpha_s(E) \times E(r) dr \tag{12}$$

In order to estimate the gain factor for the detector at both temperatures, the electric field distribution, which is geometry-dependent, should be identified in the different shapes of the detectors.

Since the distributions of the electric field under two temperatures are near the same under the same voltage in the strip detector, which can be carried out with the formula(9), the same pattern is assumed to be the tenet for the P-type point contact(PPC) detector, meaning that in our case, the electric field distribution is voltage-dependent and temperature-independent.

The electric field distribution in FIG13, which is given by the Akash report(2018-08-09), is utilized in these studies. Since there is no direct result for the electric field under a bunch of the voltages in the PPC detector, the extrapolation with the strip detector is implemented. The relation in the following formula can be employed to predict the electric field under the different voltage in the PPC detector:

$$\text{Strip detector } \frac{E_{3500V}}{E_{xV}} = \text{PPC detector} \frac{E_{3500V}}{E_{xV}} \tag{13}$$

x is the desired voltage.

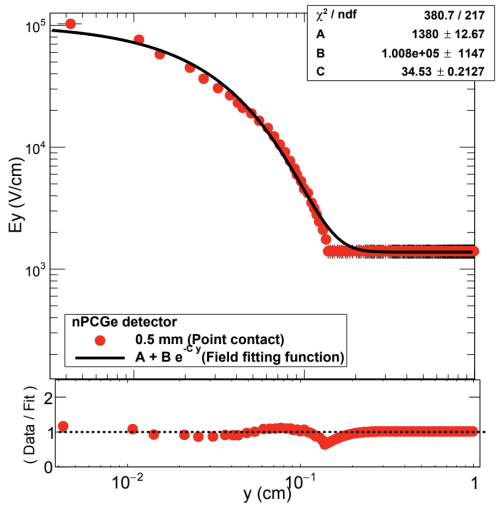

FIG. 13. The electric field distribution as a function of the radius.

After fully plotting out the electric field distribution in the PPC detector, incorporating with the ionization rate portrayed in FIG.5, the predictions for gains under both temperatures can be yielded as demonstrated in FIG.14. The small conclusion framed by this plot is that the lower the temperature we use, the lower the voltage should be applied to the crystal for achieving the same gain below 1000. Furthermore, after zooming in the region from G=1 to G=3, which is exhibited in FIG.15, the clear point at 3500V for initiating the generation of the internal amplification can be observed under 77K. At 4K,1500V is claimed to kick off the process of the internal amplification.

Albeit the lower voltage is required to attain the same gain at the lower temperature, the breakdown phenomenon, which can arise to havoc the crystal as the applied voltage exceeds the critical one, so called "breakdown voltage", should be well recognized for preventing our detector from being exterminated.

B. Electrical Breakdown

The electrical breakdown can not only alter the electrical properties of the Ge atoms permanently, but also give rise to the grave damage to the crystal, resulting in our effort to grow the available crystal is wrecked. Therefore, the theoretical forecast on the breakdown voltage should be explored ahead of time for preserving our detector from being broken.

E_{ds} obeys the following formula[15]:

$$E_{ds}(n,T) = C \times \sqrt[3]{\frac{nT}{2^n}} \tag{14}$$

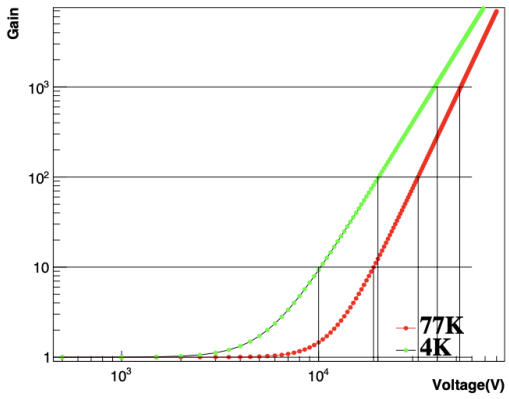

FIG. 14. The gain factor as a function of the voltage under these two temperatures.

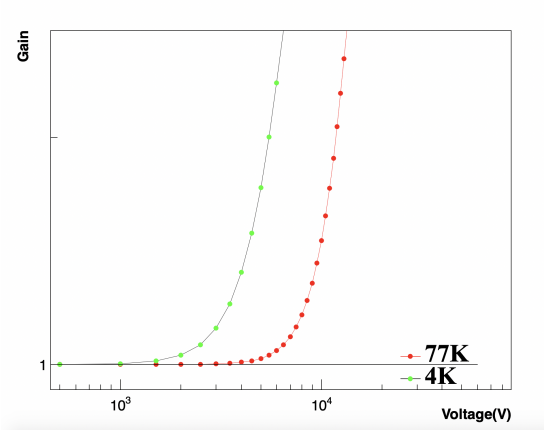

FIG. 15. The gain factor as a function of the voltage under these two temperatures.

C is a constant determined by the experiment, T is the temperature, and n is the gain factor for the amplification of electrical breakdown. If $n > 1$, it means that the electrical breakdown is opened up under the high electric field.

In FIG.16[15], it shows that the breakdown electric field for Ge at 300K is around 0.5(MV/cm) when n equals 16. With respect to the difference for E_{ds} under two different temperatures, the calculation can be made as follows:

$$E_{ds}(T) = 0.6 \times \sqrt[3]{\frac{1 \times T \times 2^{16}}{16 \times 300 \times 2^1}}(MV/cm) \tag{15}$$

Since the same gain(Gain<=1000) can be accomplished with the lower voltage at 4K as shown in FIG.14, along with the lower breakdown voltage as depicted above, the $\frac{V}{V_{BD}}$ is introduced to compare how easily the breakdown could happen to the crystal at two temperatures relatively.

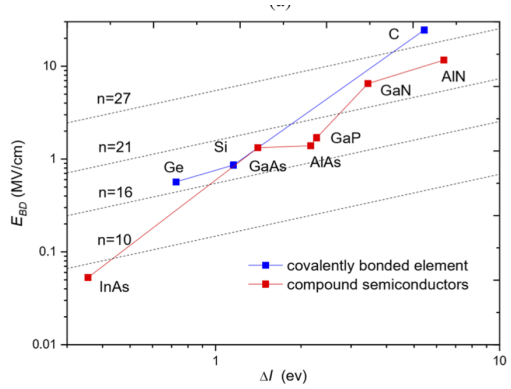

FIG. 16. ΔI is the bandgap of the material, n is the gain factor, E_{BD} is the electrical strength.

As a result of the highest electric field streaming in the detector can dictate the occurrence of the electrical breakdown, the highest electric field under the different voltage should be fully understood. In FIG.17, the electric field at r=0.05mm, where is the place on the surface of the contact, is shown as the supreme electric field in the detector under the corresponding voltage applied to the crystal. After using the formula(15) to calculate the breakdown E_{ds} under two temperatures, the matching voltage giving rise to the breakdown electric field can be grabbled by FIG.17.

In the end, as the voltages resulting in the different gains have already sought in FIG.14, as well as the research on the voltages for the electrical breakdown under two temperatures are completed, next the comparison of $\frac{V}{V_{BD}}$ can be offered. In TABLE.I, it shows the special pattern: at any gain, all of the ratios at 4K are higher than 77K, meaning that the detector can breakdown more easily at 4K.

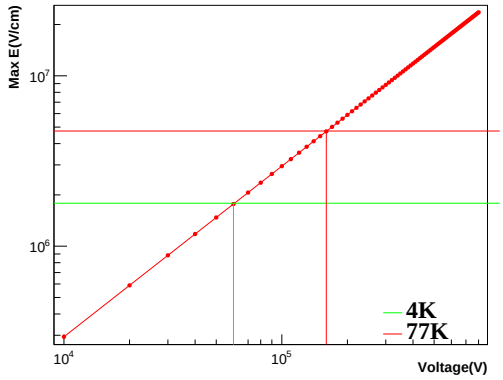

FIG. 17. The max electric field strength as a function of the voltage.

	G=10	G=100	G=1000
4K	0.16667	0.333	0.6667
77K	0.095	0.16	0.26

TABLE I. $\frac{V}{V_{BD}}$ for a variety of gains under two temperatures.

VI. CONCLUSION AND DILEMMA

1. Evidently, if the temperature is lessened to 4K, the leakage currents will be subsided to the level that those contributions to the background can be entirely ignored.

2. Some strengths aren't always advantages. Even though the same gain can be achieved with the lower voltage at 4K, the crystal should endure the risk of the lower breakdown voltage.

3. Now the experiment under 4K is anticipated to produce the first version of germanium internal amplification.

VII. TO BE CONTINUED....

VIII. ACKNOWLEDGEMENT

Thanks to Prof. Henry Wong at IoPAS on guiding me through the whole studies and providing me a lot of extraordinary advice for the direction of many issues. And thanks to Prof. Dongming on answering me most of the problems originating from the published paper and assisting me see whether the physical concepts I summarize are right.

[1] D. Neamen, *Semiconductor Physics And Devices*, 3rd ed. (McGraw-Hill, Inc., USA, 2002).

[2] C. Jacoboni, F. Nava, C. Canali, and G. Ottaviani, Phys. Rev. B **24**, 1014 (1981).

[3] D. M. Riffe, J. Opt. Soc. Am. B **19**, 1092 (2002).
[4] T. Lackner, Solid-State Electronics **34**, 33 (1991).
[5] Since the value of the mean free path is set a constant for a given temperature in the pioneer paper, we use 490nm for 77K and.
[6] W. Z. Wei, L. Wang, and D. M. Mei, JINST **12** (04), P04022, arXiv:1602.08005 [physics.ins-det].
[7] A. S. Starostin and A. G. Beda, Physics of Atomic Nuclei **63**, 1297 (2000).
[8] H. Chen, P. Verheyen, P. De Heyn, G. Lepage, J. De Coster, S. Balakrishnan, P. Absil, G. Roelkens, and J. Van Campenhout, Journal of Applied Physics **119**, 213105 (2016), https://doi.org/10.1063/1.4953147.
[9] W.-Z. Wei, X.-H. Meng, Y.-Y. Li, J. Liu, G.-J. Wang, H. Mei, G. Yang, D.-M. Mei, and C. Zhang, Journal of Instrumentation **13** (12), P12026.
[10] Q. Looker, M. Amman, and K. Vetter, Nuclear Instruments and Methods in Physics Research Section A: Accelerators, Spectrometers, Detectors and Associated Equipment **777**, 138 (2015).
[11] S. Li, *Semiconductor Physical Electronics* (Springer-Verlag, Berlin, Heidelberg, 2006).
[12] A. Milnes and D. Feucht, in *Heterojunctions and Metal Semiconductor Junctions*, edited by A. Milnes and D. Feucht (Academic Press, 1972) pp. 171 – 200.
[13] P. J. Ker, A. R. J. Marshall, A. B. Krysa, J. P. R. David, and C. H. Tan, IEEE Journal of Quantum Electronics **47**, 1123 (2011).
[14] S. Bhattarai, R. Panth, W. Z. Wei, H. Mei, D. M. Mei, M. S. Raut, P. Acharya, and G. J. Wang, Eur. Phys. J. C **80**, 950 (2020), arXiv:2002.07707 [physics.ins-det].
[15] L. Zhao, AIP Advances **10**, 025003 (2020).